# Supplementary Information

# Hydrogen-bonded assemblies of iron(II) spin crossover complexes

**Verónica Jornet-Mollá, Marina I. Rodríguez-Tarrazó, Miquel J. Dolz Lozano, Carlos Giménez-Saiz and Francisco M. Romero***

**Table S1** Octahedral distortion parameters of the $Fe^{2+}$ cations present in compounds **1-3** obtained from X-ray data.

| | **1** | **2** | **3** |
|---|---|---|---|
| $\varphi$ / deg | 178.36(16) | 177.89(15) | 164.94(11) |
| $\Sigma$ / deg | 99(2) | 98(2) | 144(1) |

**Table S2.** Intermolecular hydrogen bonds in the crystal structure of **1**.[a]

| D–H···A | d(D–H)/Å | d(H···A)/Å | d(D···A)/Å | <(D–H···A)/deg |
|---|---|---|---|---|
| N1–H1N···O2_#4 | 0.88(2) | 1.85(3) | 2.675(5) | 156(5) |
| N5–H5N···O1_#5 | 0.90(2) | 1.80(3) | 2.696(5) | 177(5) |
| N6–H6N···O1W | 0.89(3) | 1.95(3) | 2.769(5) | 152(5) |
| N10–H10N···O4 | 0.89(2) | 1.84(3) | 2.728(4) | 174(4) |
| O1W–H1W1···O4_#6 | 0.82(2) | 1.86(3) | 2.667(5) | 167(6) |
| O2W–H2W1···O3 | 0.84(3) | 2.09(3) | 2.921(5) | 171(5) |
| O2W–H2W2···O5W | 0.81(3) | 2.06(3) | 2.859(6) | 166(6) |
| O3W–H3W1···O1_#7 | 0.78(2) | 2.11(3) | 2.884(5) | 177(6) |
| O3W–H3W2···O7W | 0.79(2) | 1.98(3) | 2.721(5) | 156(5) |
| O4W–H4W1···O8W_#1 | 0.91(3) | 2.00(4) | 2.763(6) | 141(6) |
| O4W–H4W2···O1W | 0.88(3) | 1.99(3) | 2.857(6) | 169(7) |
| O5W–H5W1···O3W_#8 | 0.86(3) | 2.00(3) | 2.836(6) | 164(6) |
| O5W–H5W2···O8W | 0.86(3) | 1.95(3) | 2.791(6) | 165(6) |
| O6W–H6W1···O4W_#9 | 0.83(3) | 2.04(5) | 2.803(6) | 152(9) |
| O6W–H6W2···O2 | 0.82(3) | 2.16(6) | 2.908(6) | 151(10) |
| O7W–H7W1···O4W_#2 | 0.84(3) | 2.01(3) | 2.833(7) | 167(4) |
| O7W–H7W2···O3 | 0.83(3) | 1.95(3) | 2.728(5) | 157(7) |
| O8W–H8W1···O9W_#10 | 0.85(2) | 1.91(3) | 2.738(6) | 165(6) |
| O8W–H8W2···O7W | 0.87(2) | 1.96(3) | 2.820(6) | 168(5) |
| O9W–H9W1···O6W_#11 | 0.86(3) | 1.96(3) | 2.795(7) | 163(6) |
| O9W–H9W2···O2W_#7 | 0.86(3) | 2.13(5) | 2.825(6) | 137(7) |

[a]Symmetry transformations used to generate equivalent atoms:

#1 $-x+1/2, -y+1, z+1/2$ #2 $-x+1, y+1/2, -z+3/2$ #3 $-x+1/2, -y+2, z+1/2$
#4 $x+1/2, -y+3/2, -z+2$ #5 $x+1, y, z$ #6 $-x+1, y-1/2, -z+3/2$
#7 $-x, y-1/2, -z+3/2$ #8 $x-1/2, -y+3/2, -z+1$ #9 $x-1/2, -y+3/2, -z+2$
#10 $-x+1/2, -y+1, z-1/2$ #11 $x, y-1, z$

**Table S3** Intermolecular hydrogen bonds in the crystal structure of **2**.[a]

| **D–H···A** | **d(D–H)/Å** | **d(H···A)/Å** | **d(D···A)/Å** | **<(D–H···A)/deg** |
|---|---|---|---|---|
| N1–H1N···O2_#1 | 0.901(19) | 1.83(3) | 2.688(5) | 157(5) |
| N5–H5N···O3W | 0.901(19) | 1.74(2) | 2.637(5) | 171(5) |
| N6–H6N···O6_#2 | 0.895(19) | 1.82(2) | 2.702(5) | 166(5) |
| N10–H10N···O1W_#3 | 0.901(18) | 1.82(2) | 2.694(5) | 163(4) |
| O5–H5O···O1_#4 | 1.12(7) | 1.38(7) | 2.499(4) | 179(6) |
| O1W–H1W1···O2W | 0.802(18) | 1.90(2) | 2.697(4) | 171(5) |
| O1W–H1W2···O5W | 0.824(19) | 1.83(2) | 2.644(5) | 169(5) |
| O2W–H2W1···O4_#5 | 0.825(18) | 1.88(2) | 2.702(4) | 176(4) |
| O2W–H2W2···O4 | 0.818(18) | 2.04(2) | 2.842(4) | 166(6) |
| O3W–H3W1···O4W | 0.832(19) | 1.87(2) | 2.686(5) | 167(6) |
| O3W–H3W2···O2 | 0.823(19) | 1.987(19) | 2.796(5) | 168(5) |
| O4W–H4W1···O1W | 0.838(19) | 1.96(2) | 2.775(5) | 164(6) |
| O4W–H4W2···O3 | 0.832(19) | 1.987(19) | 2.818(5) | 177(5) |
| O5W–H5W1···O3_#1 | 0.839(19) | 1.87(2) | 2.703(5) | 172(5) |
| O5W–H5W2···O2W_#6 | 0.821(18) | 2.05(2) | 2.836(5) | 160(4) |

[a] Symmetry transformations used to generate equivalent atoms:

#1 $x-1, y, z$ #2 $x, y, z+1$
#3 $-x+1, -y, -z+1$ #4 $x-1/2, -y+1/2, z-1/2$
#5 $-x+2, -y, -z$ #6 $-x+1, -y, -z$

**Table S4** Intermolecular hydrogen bonds in the crystal structure of **3**.[a]

| **D–H···A** | **d(D–H)/Å** | **d(H···A)/Å** | **d(D···A)/Å** | **<(D–H···A)/deg** |
|---|---|---|---|---|
| N1–H1N···O1W | 0.87(2) | 1.84(3) | 2.713(5) | 173(5) |
| N5–H5N···O1_#2 | 0.89(3) | 1.76(3) | 2.637(4) | 169(6) |
| N6–H6N···O3W_#3 | 0.85(2) | 1.95(3) | 2.781(5) | 165(5) |
| N10–H10N···O2_#4 | 0.88(2) | 1.81(3) | 2.676(4) | 166(5) |
| O1W–H1W1···O1_#5 | 0.81(2) | 2.03(2) | 2.821(4) | 167(5) |
| O1W–H1W2···O2W | 0.83(2) | 1.99(3) | 2.814(5) | 170(6) |
| O2W–H2W1···O4_#4 | 0.85(2) | 1.93(3) | 2.779(5) | 172(6) |
| O2W–H2W2···O4W_#4 | 0.86(2) | 1.96(3) | 2.799(6) | 169(5) |
| O3W–H3W1···O4_#6 | 0.84(2) | 1.80(3) | 2.626(5) | 167(4) |
| O3W–H3W2···O6W | 0.84(3) | 1.77(4) | 2.564(10) | 156(6) |
| O4W–H4W1···O3_#7 | 0.83(3) | 1.93(3) | 2.736(6) | 163(7) |
| O4W–H4W2···O5W_#8 | 0.87(2) | 2.18(4) | 2.934(5) | 146(6) |
| O5W–H5W1···O3W | 0.85(2) | 2.00(3) | 2.840(6) | 168(4) |
| O6W–H6W1···O3_#5 | 0.81(3) | 1.77(5) | 2.550(9) | 160(10) |
| O6W–H6W2···O3_#6 | 0.80(3) | 2.18(7) | 2.849(7) | 141(11) |

[a] Symmetry transformations used to generate equivalent atoms:

#1 $x, y - 1, z + 1$ #2 $-x + 2, -y, z$ #3 $-x + 3/2, y - 1/2, -z + 1$
#4 $x, y - 1, z$ #5 $-x + 2, -y + 1, z$ #6 $x, y, z + 1$
#7 $x, y + 1, z$

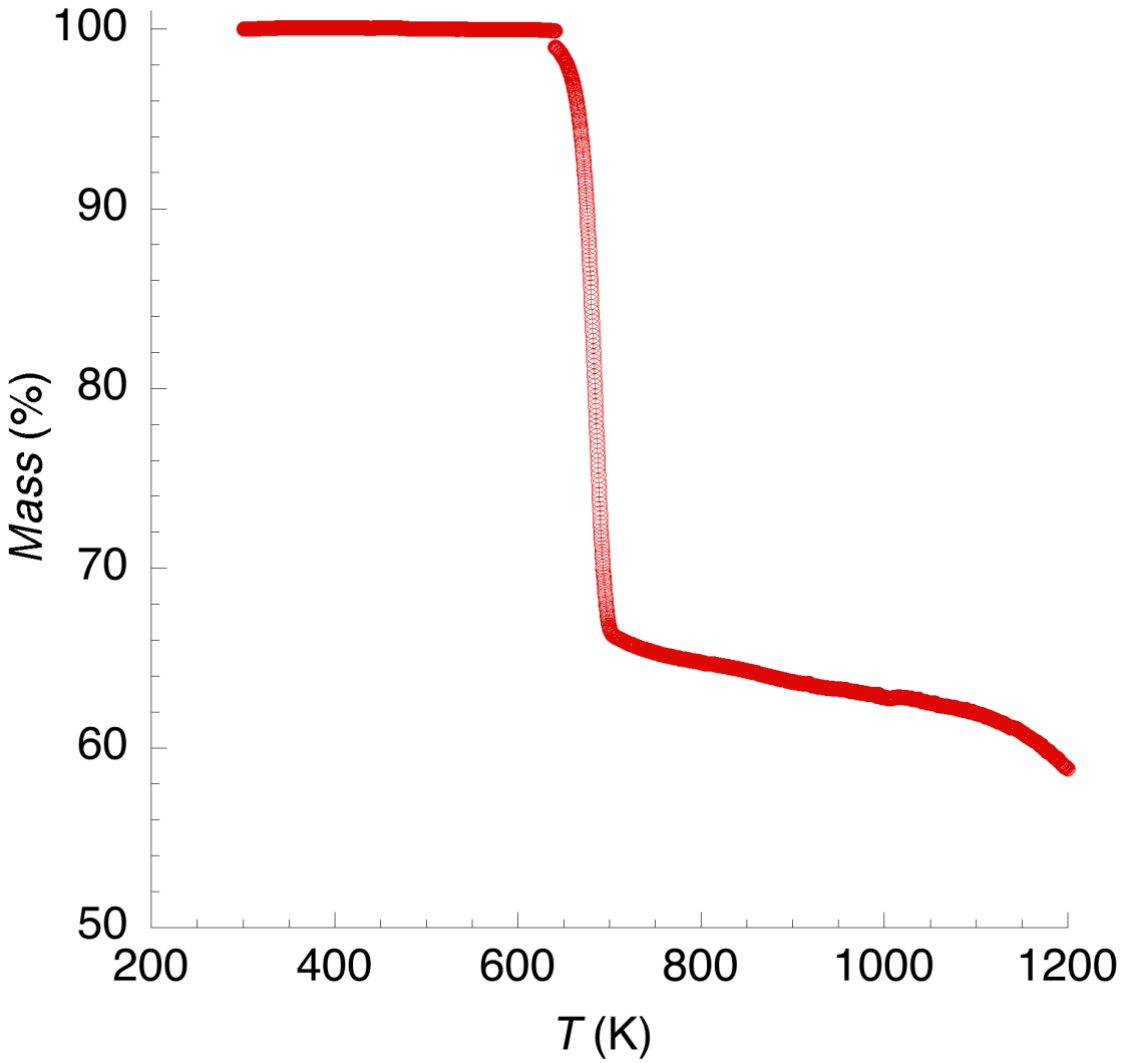


**Fig. S1.** Thermogravimetric analysis of $Ag_2(BPDC)$, BPDC = $C_{14}H_8O_4$. The plot confirms the anhydrous character of this salt.

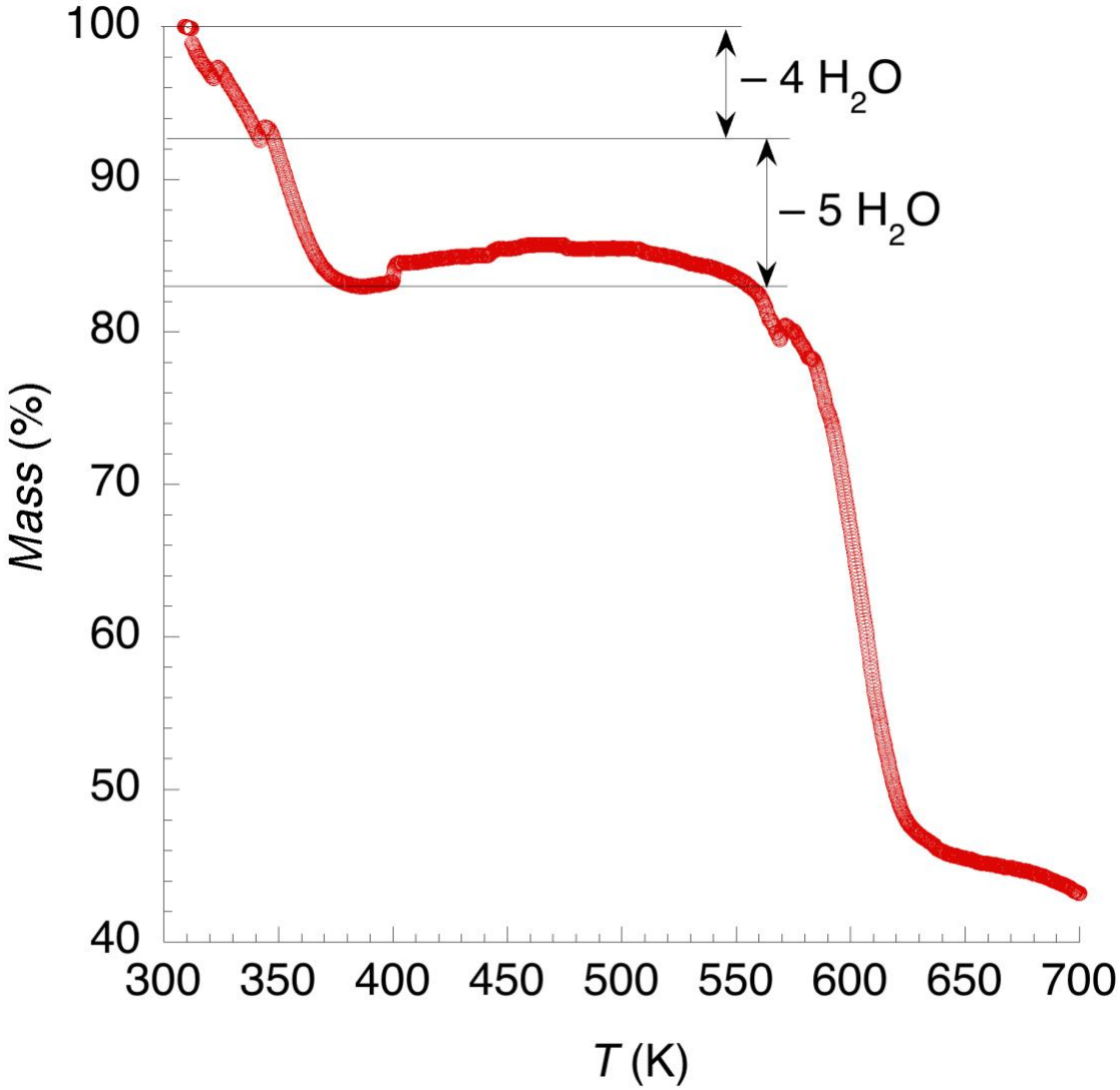


**Fig. S2.** Thermogravimetric analysis of $[Fe(bpp)_2](ADC)\cdot 9H_2O$ (**1**), bpp = $C_{11}H_9N_5$, ADC = $C_{16}H_8O_4$.

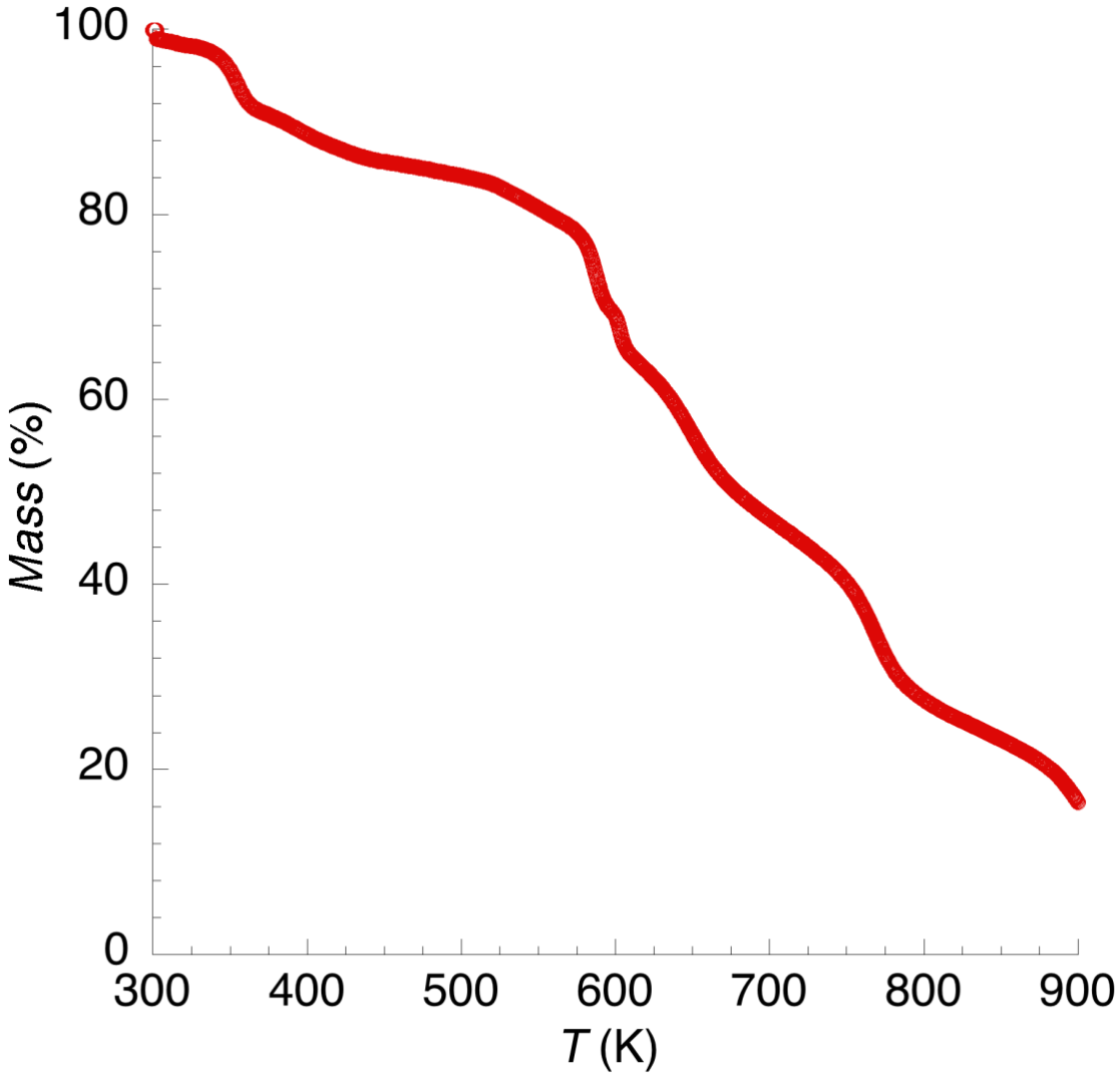


**Fig. S3.** Thermogravimetric analysis of $[Fe(bpp)_2](HBTC)\cdot 5H_2O$ (**2**), bpp = $C_{11}H_9N_5$, BTC = $C_9H_3O_6$..

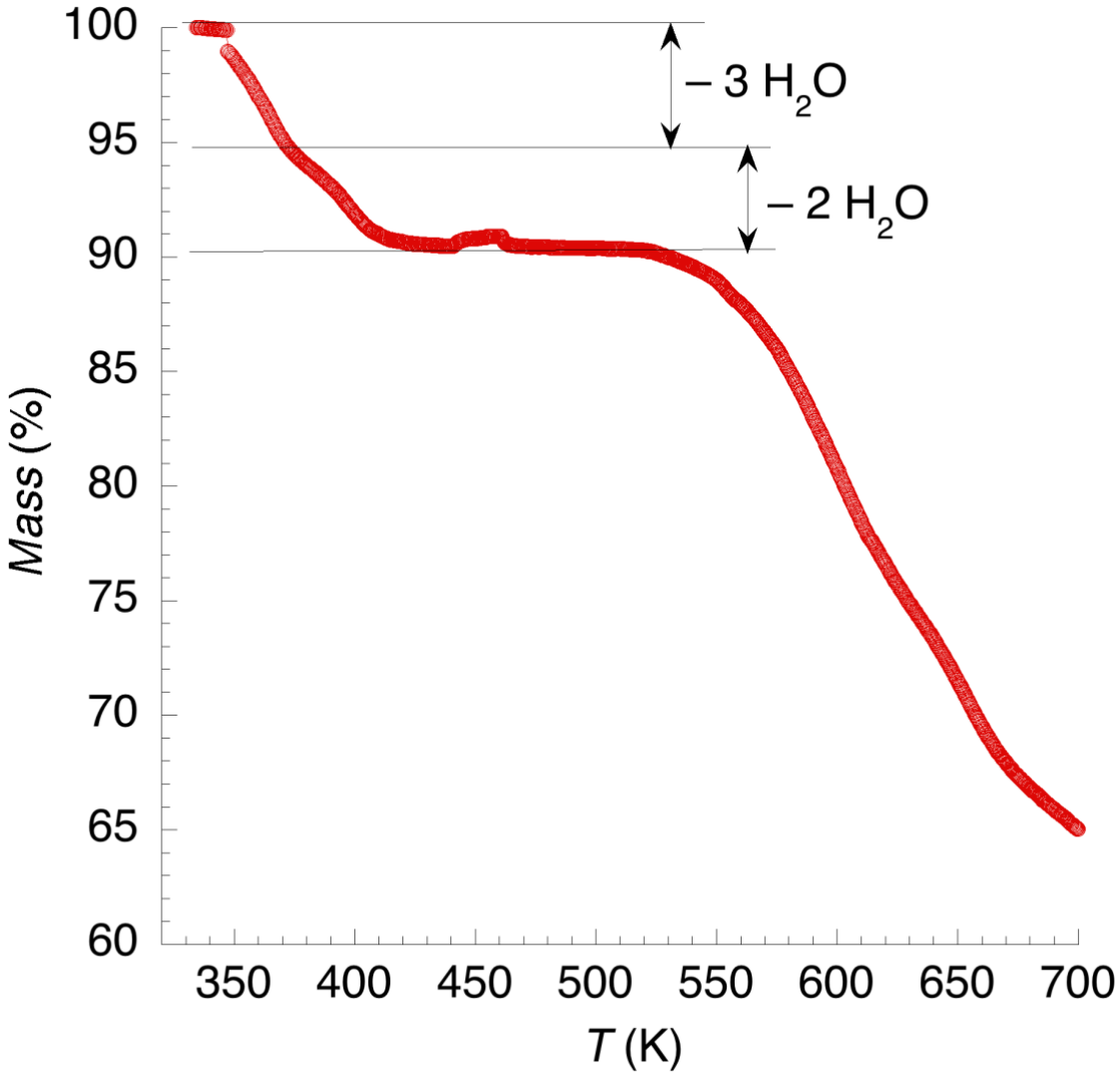


**Fig. S4.** Thermogravimetric analysis of $[Fe(bpp)_2](BPDC)\cdot 5H_2O$ (**3**), bpp = $C_{11}H_9N_5$, BPDC = $C_{14}H_8O_4$.

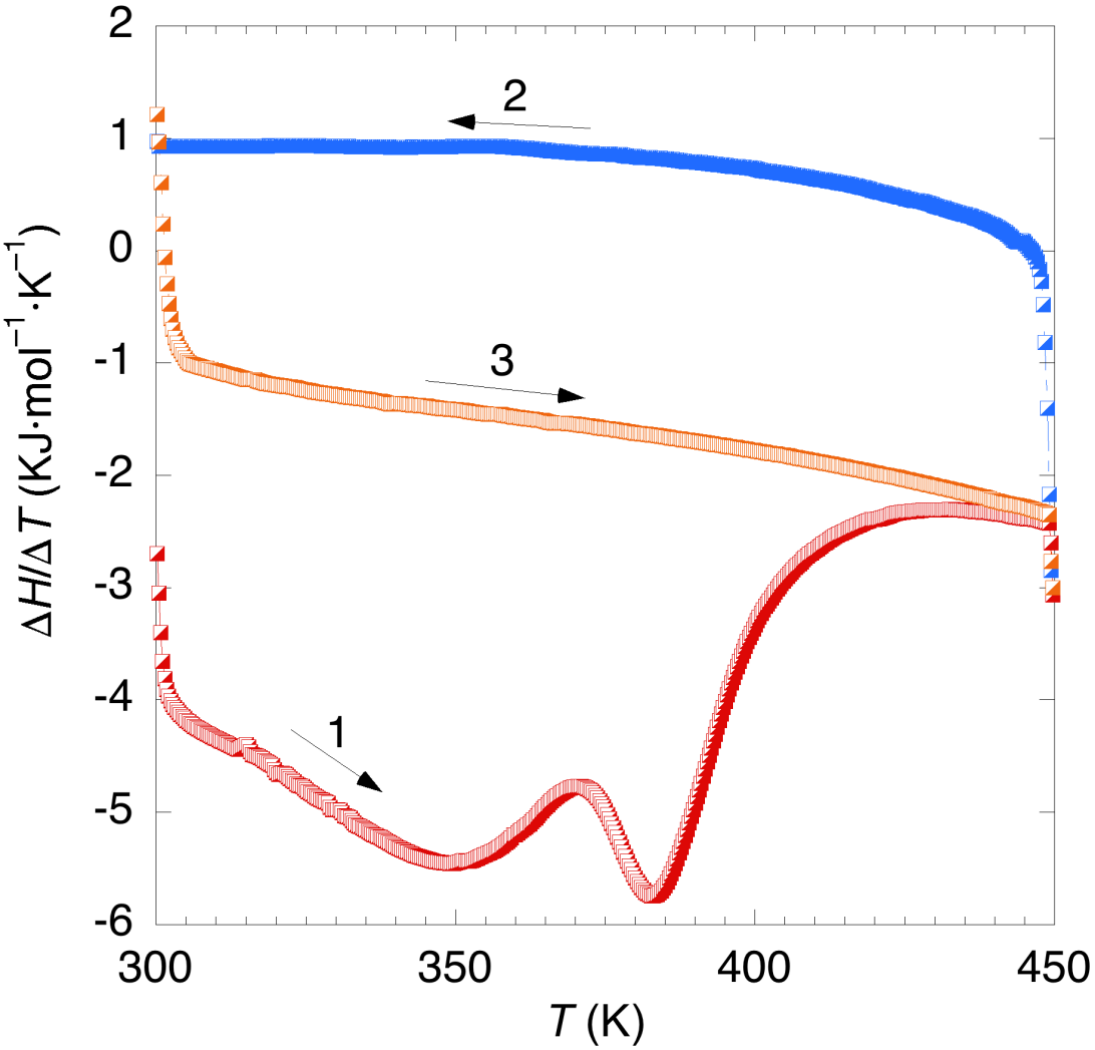


**Fig. S5.** Differential scanning calorimetry of **1**. Curve 1: first heating (dehydration process). Curve 2: first cooling. Curve 3: second heating.

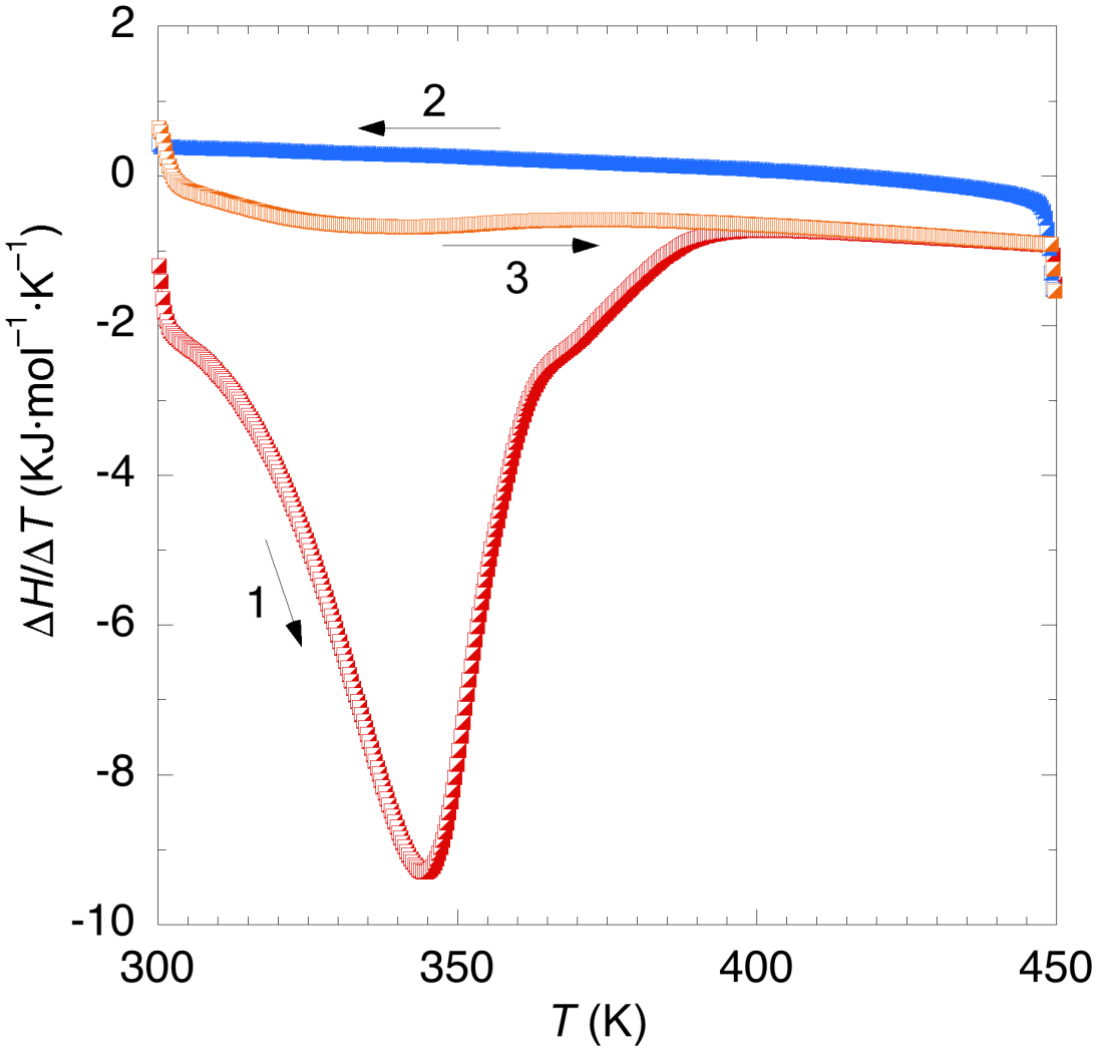


**Fig. S6.** Differential scanning calorimetry of **2**. Curve 1: first heating (dehydration process). Curve 2: first cooling. Curve 3: second heating.

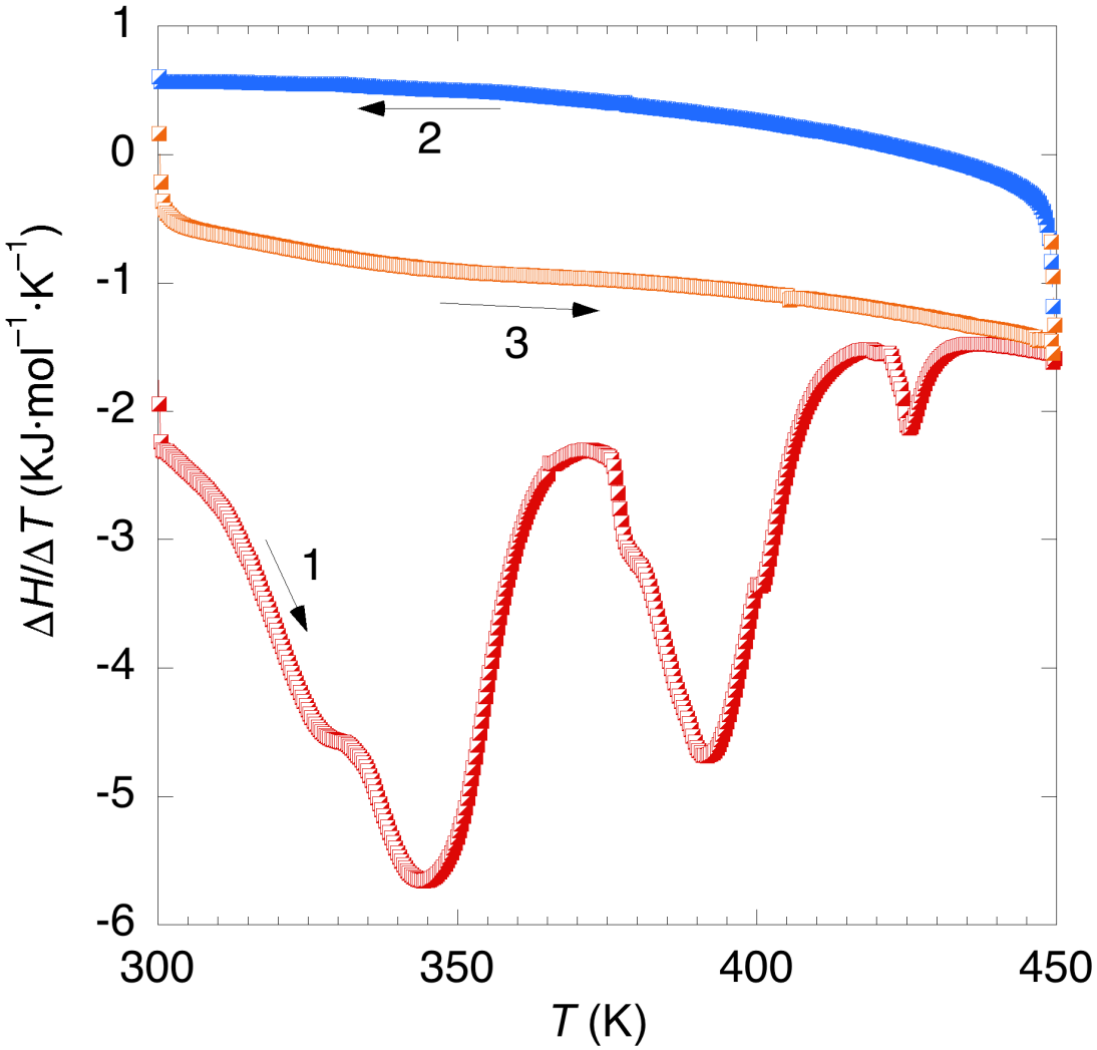


**Fig. S7.** Differential scanning calorimetry of **3**. Curve 1: first heating (dehydration process). Curve 2: first cooling. Curve 3: second heating.

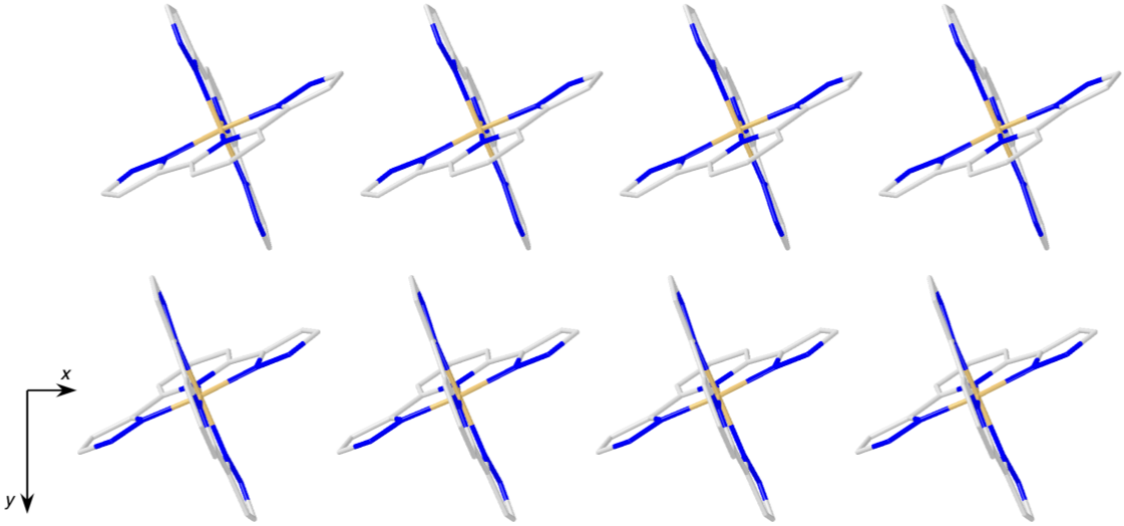


**Fig. S8.** View of the crystal structure of **2** along the *b* axis, emphasizing the $\pi$-$\pi$ stacking interactions (shown as dashed lines) between neighbouring $[Fe(bpp)_2]^{2+}$ cations. Double chains of cations stacked along the *x* direction can be seen. Water molecules and HBTC anions are omitted.

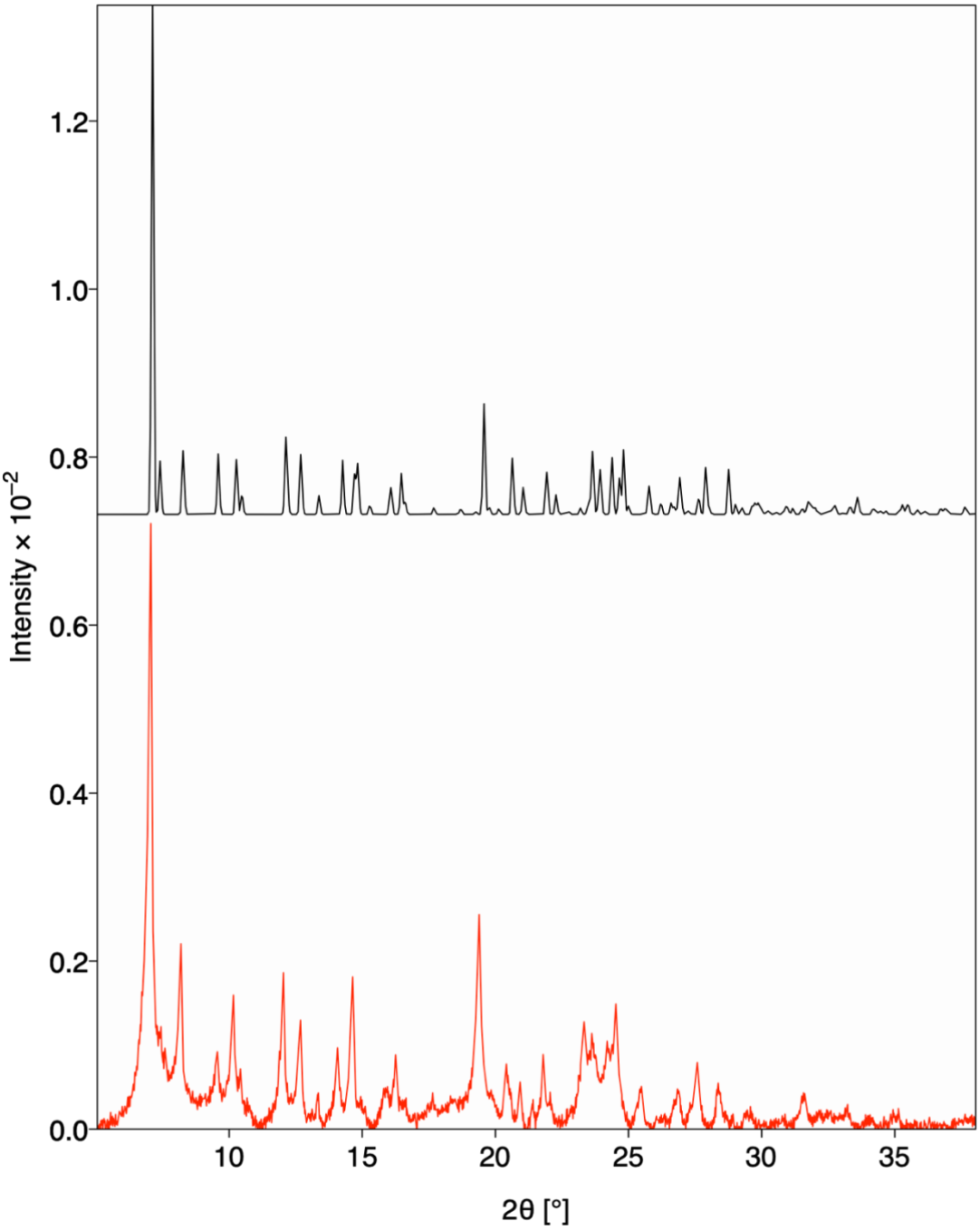


**Fig. S9.** Comparison of the X-ray powder diffractogram of **1** (red line) with the simulation obtained from single crystal data (black line).

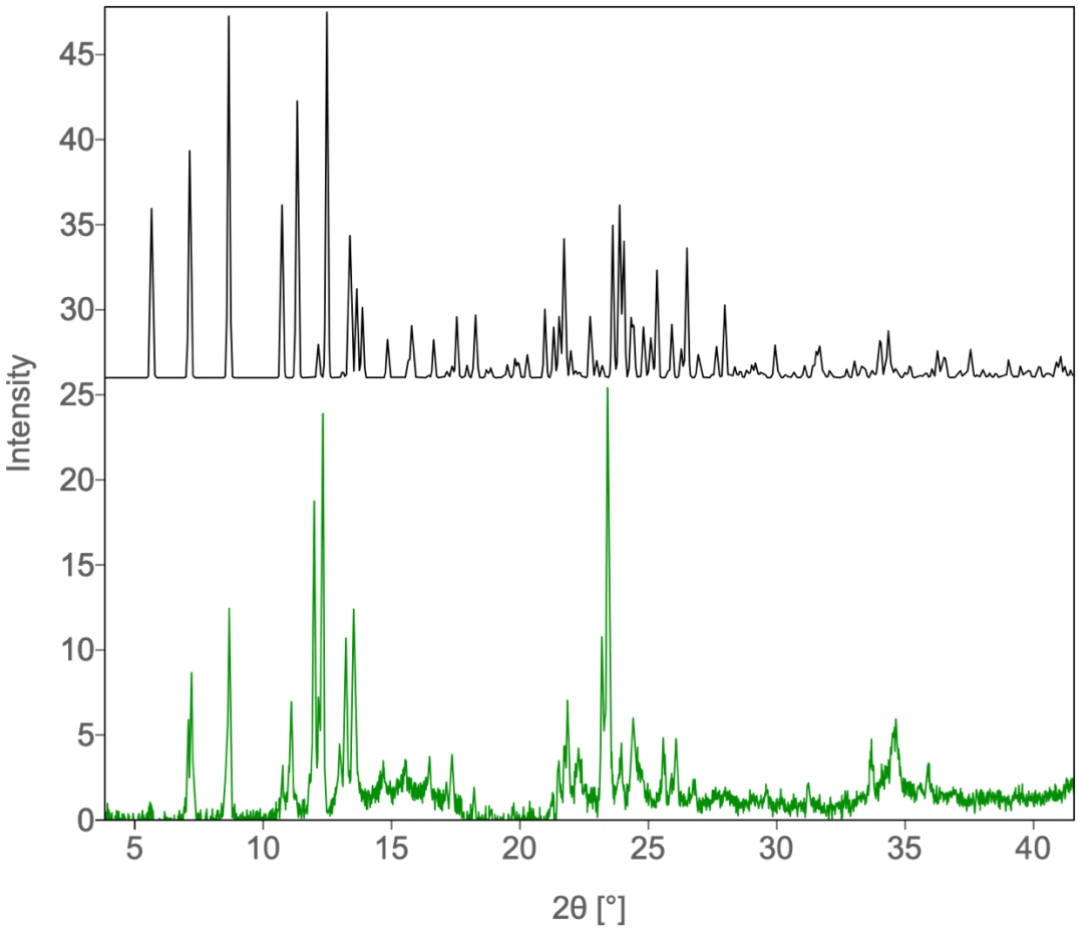


**Fig. S10.** Comparison of the X-ray powder diffractogram of **2** (green line) with the simulation obtained from single crystal data (black line).

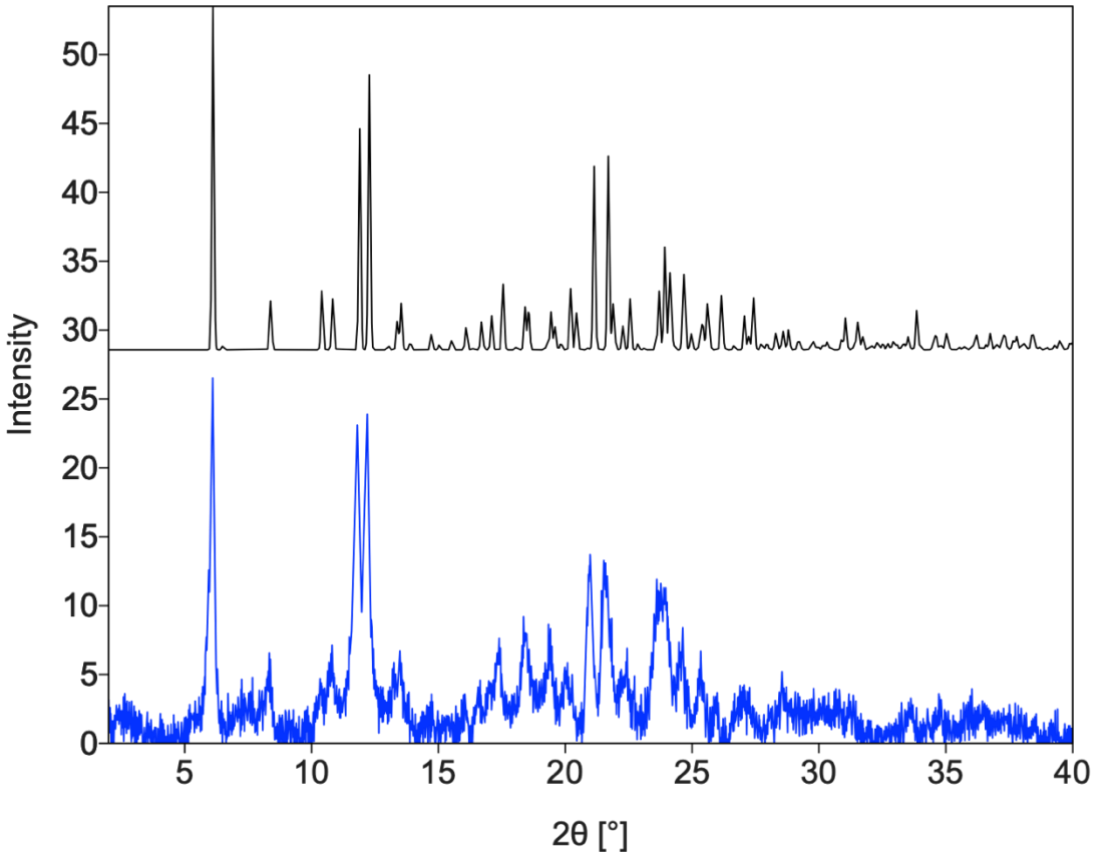


**Fig. S11.** Comparison of the X-ray powder diffractogram of **3** (blue line) with the simulation obtained from single crystal data (black line).